

Wintertime Nocturnal Temperature Distribution Based on Spatially High Density Observation Data in the Tokyo Metropolitan Area under Clear Sky and Weak Wind Conditions

SETO, Yoshihito / Takahashi, Hideo / YOKOYAMA, Hitoshi /
SHIMIZU, Shogo / YAMATO, Hiroaki

(出版者 / Publisher)

Japan Climatology Seminar

(雑誌名 / Journal or Publication Title)

Japanese progress in climatology / Japanese progress in climatology

(巻 / Volume)

2014

(開始ページ / Start Page)

57

(終了ページ / End Page)

64

(発行年 / Year)

2014-12

Reprinted from *Journal of Geography*. Vol. 132–(2), pp. 189~210, 2014.

**Wintertime Nocturnal Temperature Distribution Based on Spatially High Density
Observation Data in the Tokyo Metropolitan Area under Clear Sky
and Weak Wind Conditions**

Hideo TAKAHASHI*, Shogo SHIMIZU*, Hiroaki YAMATO**,
Yoshihito SETO* and Hitoshi YOKOYAMA***

[Received 27 October, 2013; Accepted 19 January, 2014]

Abstract

Tokyo—one of the largest cities in the world—exhibits intensive urban land use, urban sprawl, and high anthropogenic heat exhaustion, which produce characteristic urban temperature distributions. Typical features of the nocturnal temperature distribution from November to February under conditions of clear skies and weak winds were analyzed for the Tokyo metropolitan-ward area using data from spatially high-density observations from the Automated Meteorological Data Acquisition System (AMeDAS) of the Japan Meteorological Agency (JMA), municipal air pollution monitoring systems, and Extended-METROS from 2006/2007 to 2009/2010. To analyze the structure of temperature distributions in the Tokyo-ward area, hourly temperature data at 124 stations were interpolated into grid points with 1-km intervals.

When high temperatures in central Tokyo were expressed as a difference in AMeDAS temperature between central Tokyo (Otemachi) and an average of four points outside the Tokyo-ward area, the weather conditions most strongly affecting this temperature difference at 06:00 Japan Standard Time (JST), prior to sunrise, were cloud amount followed by wind speed. The temperature difference at night under clear-sky and weak-wind conditions (average cloud amount of 2/10 or less and average wind speed of 3 m/s or less) generally showed an abrupt increase during the several hours before and after sunset followed by a gradual increase, reaching maximum levels before sunrise (06:00 JST). When the temperature difference before sunrise was large, the difference would evidently increase even after midnight; however, if this difference was small, it would tend to decrease after midnight.

The high temperatures in the metropolitan area were concentrated throughout the night near the southern area of Chuo ward. In particular, it is noted that several zones of steep horizontal temperature gradients were detected in the metropolitan-ward area. These zones (e.g. starting from the southern part of Saitama Prefecture, it appeared through the border between Nerima and Itabashi wards, Toshima, Shinjuku, and the area stretching from western Setagaya to the southwest) appeared during the period several hours before and after sunset, and gradually became more noticeable near sunrise. The distribution of temperature-decrease rate around sunset also showed steep horizontal gradient zones, which corresponded to regions exhibiting steep horizontal temperature gradient zones between the inner city and outer area.

Key words : urban heat island, nocturnal temperature distribution, cloud amount, wind speed, horizontal temperature gradient, Extended-METROS

* Department of Geography, Graduate School of Urban Environmental Sciences, Tokyo Metropolitan University, Hachioji, 192-0397, Japan

** Department of Integrated Science and Engineering for Sustainable Society, Faculty of Science and Engineering, Chuo University, Hachioji, 192-0393, Japan

*** Tokyo Metropolitan Research Institute for Environmental Protection, Tokyo, 136-0075, Japan

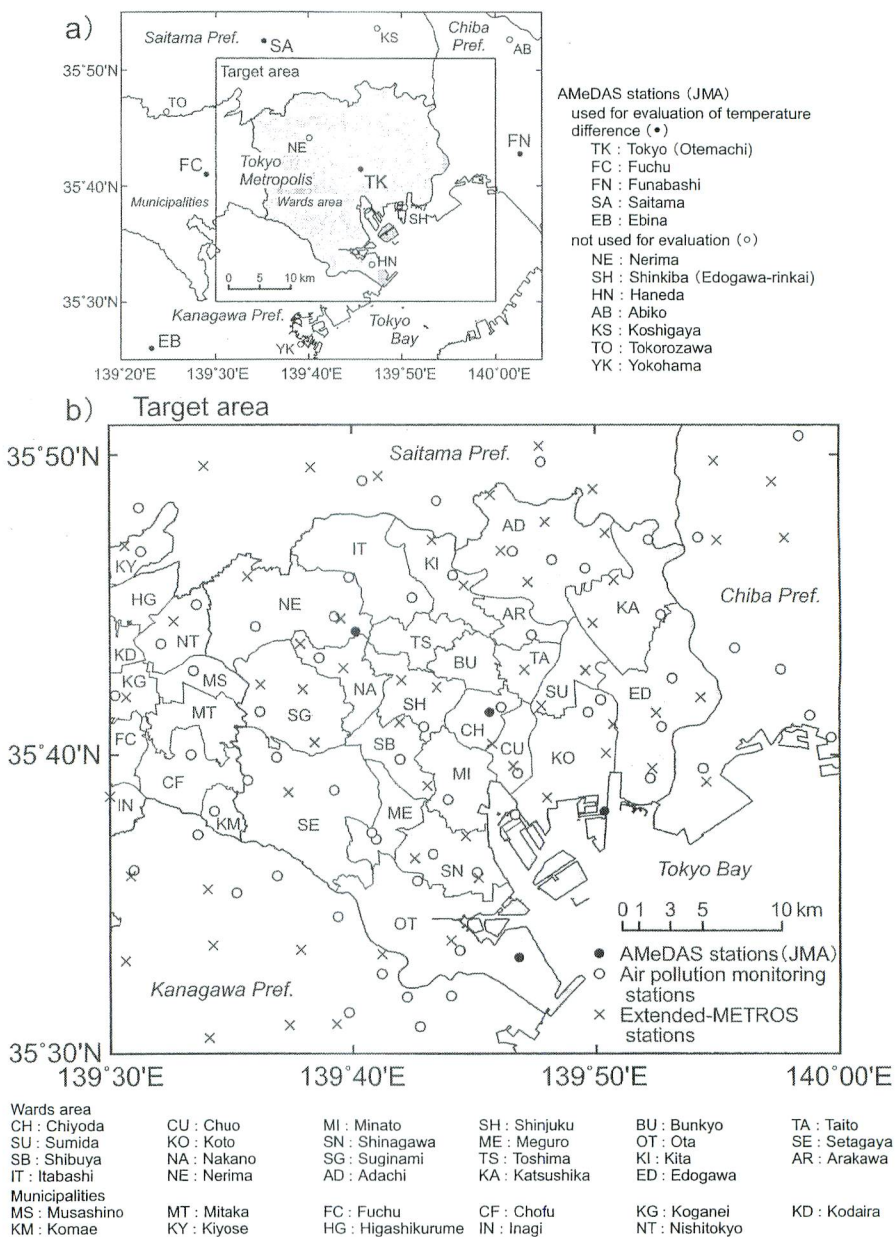


Fig. 1 Index map showing target area and locations of observation stations.

a) Target area and locations of AMeDAS stations (black circles) used for evaluating temperature differences between central Tokyo and area outside Tokyo wards (AMeDAS stations not used for evaluating temperature differences are shown with white circles), b) Locations of observation stations, and wards, and cities of Metropolitan Tokyo.

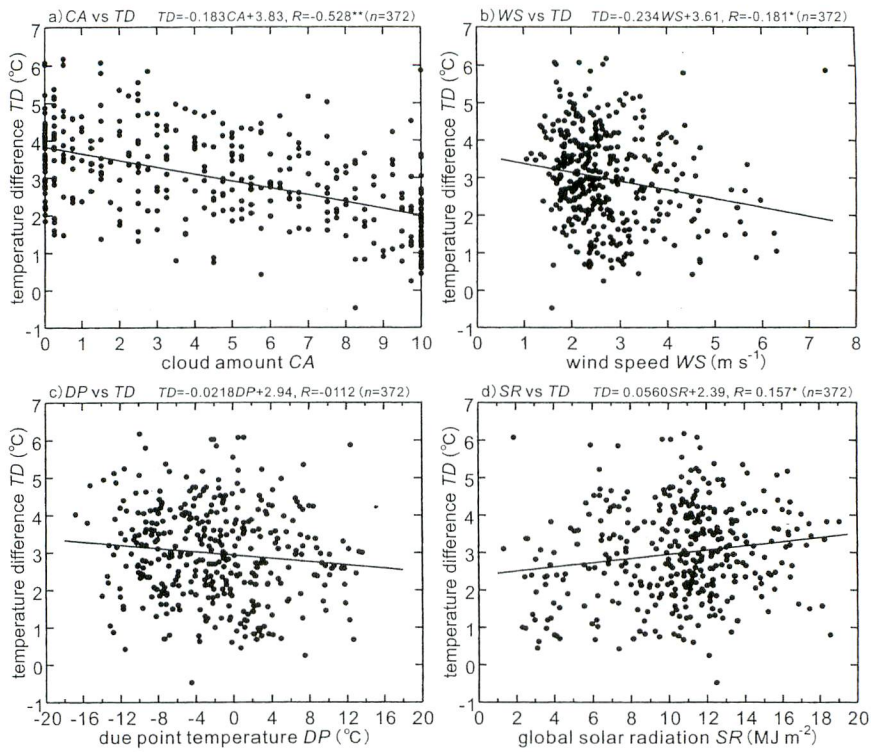


Fig. 2 Relationships between temperature difference (TD) at 06:00 JST and weather conditions.

a) Average cloud amount during the night (CA), b) Average wind speed during the night (WS), c) Average dew-point temperature during the night (DP), d) Global solar radiation during the preceding daytime (SR). Solid line in each figure represents regression line. Regression coefficients and correlation coefficient are also indicated above each figure. *Statistically significant at 5%. **Statistically significant at 1%.

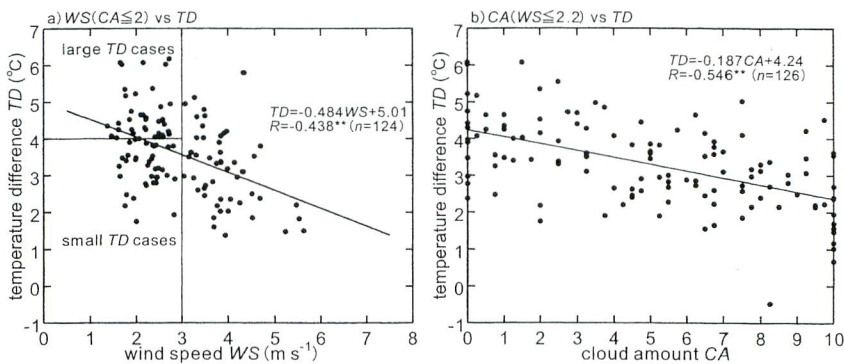


Fig. 3 Relationships between temperature difference (TD) at 06:00 JST and a) average wind speed during the night (WS) when cloud amount is low ($CA \leq 2$) and b) average cloud amount during the night (CA) when wind speed is low ($WS \leq 2.2$ m/s).

Solid line in each figure represents regression line. Regression coefficients and correlation coefficient are also indicated above each figure. **Statistically significant at 1%.

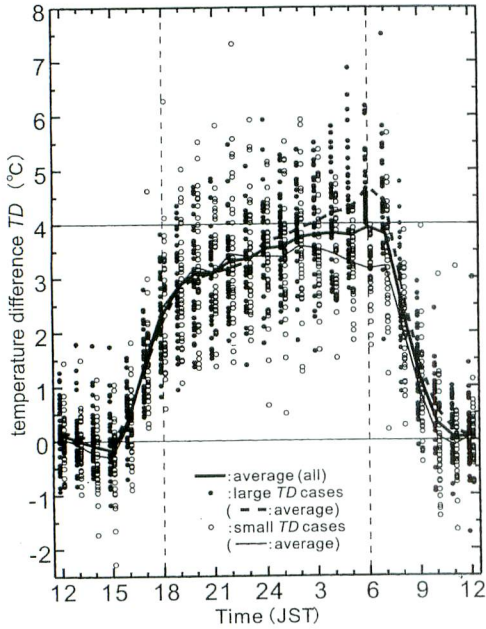


Fig. 4 Diurnal variations in temperature difference between central Tokyo and area outside Tokyo wards (*TD*).

Bold solid line indicates diurnal variations in temperature differences averaged for all clear-sky and weak-wind cases. Black and white circles show cases of large ($TD \geq 4^\circ\text{C}$) and small ($TD < 4^\circ\text{C}$) temperature differences, respectively, at 06:00 JST for clear-sky and weak-wind nights.

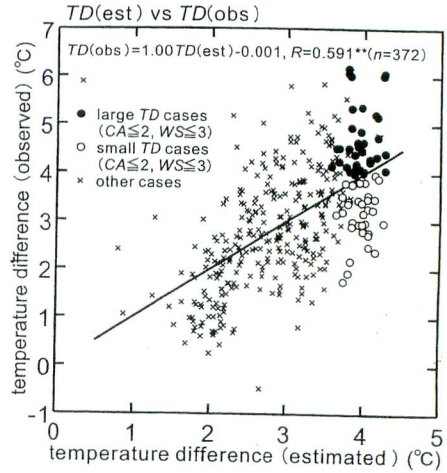


Fig. 5 Relationship between actual temperature difference, *TD* (obs) at 06:00 JST, and that evaluated from average cloud amount and wind speed during the night using a multiple regression analysis, *TD* (est).

Solid line shows regression line. Black and white circles indicate cases of large ($TD \geq 4^\circ\text{C}$) and small ($TD < 4^\circ\text{C}$) temperature differences, respectively, at 06:00 JST for clear-sky and weak-wind nights. **Statistically significant at 1%.

Table 1 Matrix showing number of clear-sky and weak-wind nights when the temperature difference at 06:00 JST was large ($TD \geq 4^\circ\text{C}$) or small ($TD < 4^\circ\text{C}$) on the day following a holiday (I) or weekday (II).

No. of days	I	II	Total
$TD \geq 4^\circ\text{C}$	12	25	37
$TD < 4^\circ\text{C}$	20	16	36
Total	32	41	73

I: days following a weekend. II: days following a weekday.

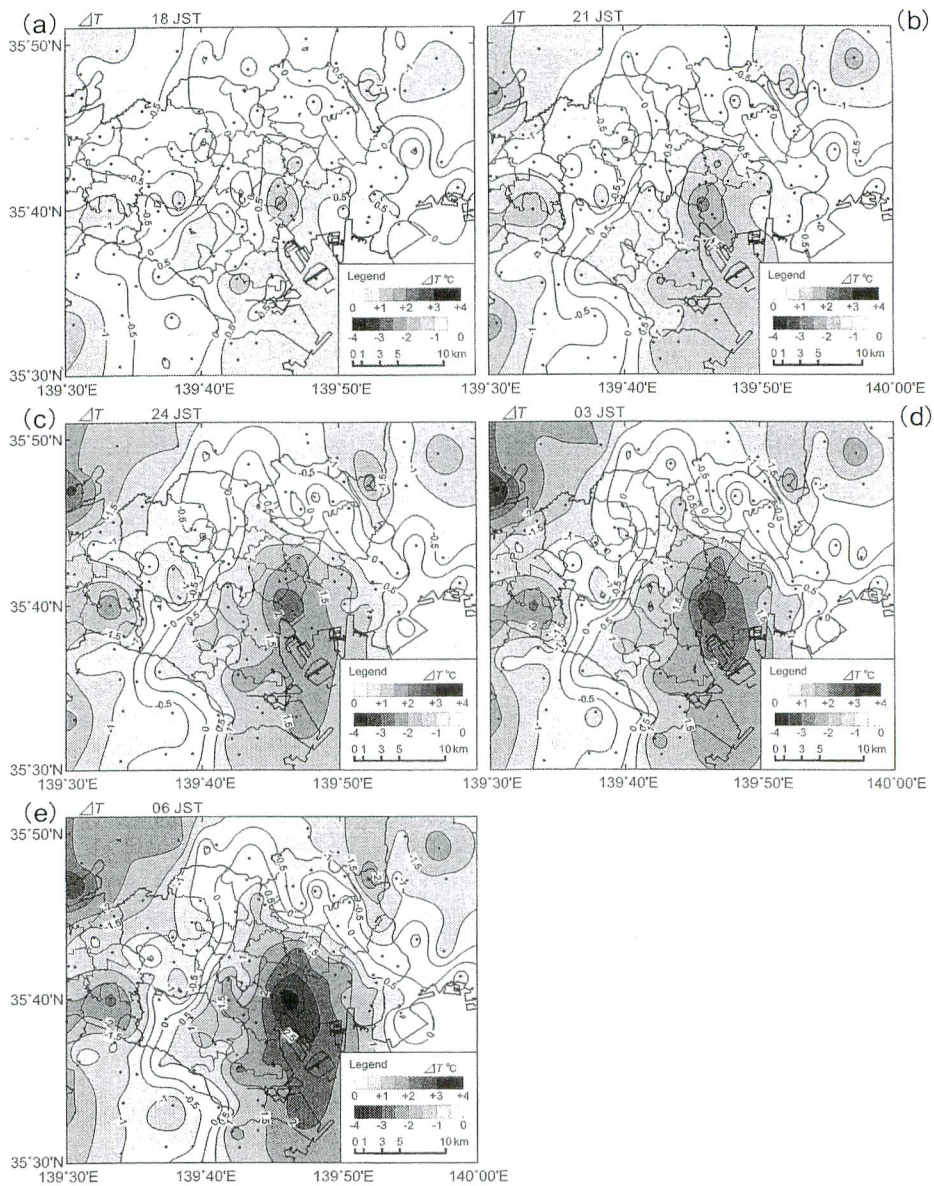


Fig. 6 Composite temperature distribution in the Tokyo-ward area and its surroundings on clear-sky and weak-wind nights with a large temperature difference between central Tokyo and area outside the Tokyo wards at 06:00 JST. (a) 18:00 JST, (b) 21:00 JST, (c) 24:00 JST, (d) 03:00 JST, (e) 06:00 JST. Temperature distribution is shown as a composite map of temperature deviation (ΔT) from spatial average temperature for the respective cases. Contour lines are drawn at every $0.5^{\circ}\text{C}/\text{h}$.

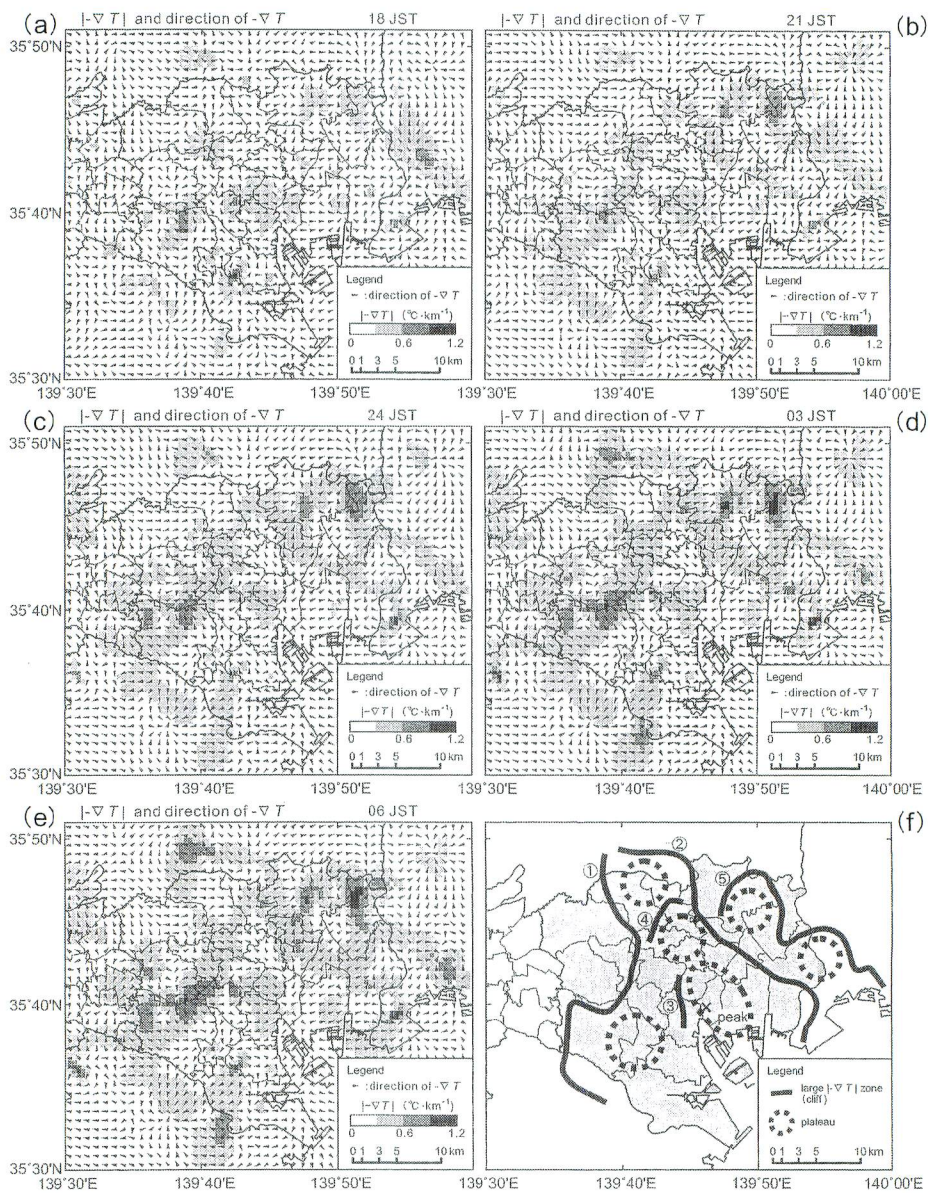


Fig. 7 Magnitude (gray scale) and direction (arrows) of composited horizontal temperature gradient ($-\nabla T$) corresponding to Fig. 6, and schematic representing the structure of the temperature distribution in the Tokyo-ward area.

(a) 18:00 JST, (b) 21:00 JST, (c) 24:00 JST, (d) 03:00 JST, (e) 06:00 JST, (f) Structure of temperature distribution. Regarding (f), bold lines indicated by ①-⑤ (see description in the abstract) are zones of large temperature gradients (cliff), and broken circles (oval) show plateau-like high-temperature areas.

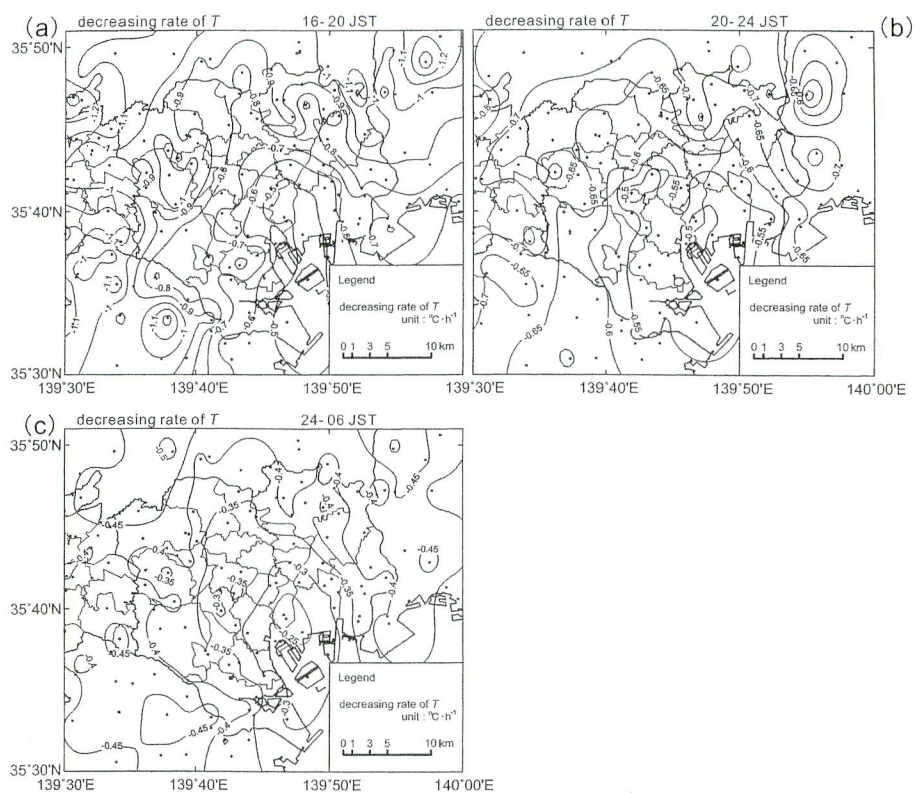


Fig. 8 Composite distribution of temperature change rate per hour ($^{\circ}\text{C}/\text{h}$) for clear-sky and weak-wind nights with a large temperature difference between central Tokyo and area outside Tokyo wards at 06:00 JST. (a) from 16:00 JST to 20:00 JST, (b) from 20:00 JST to 24:00 JST, (c) from 24:00 JST to 06:00 JST. Contour lines are drawn at every $0.1^{\circ}\text{C}/\text{h}$ in (a) and $0.05^{\circ}\text{C}/\text{h}$ in (b) and (c).

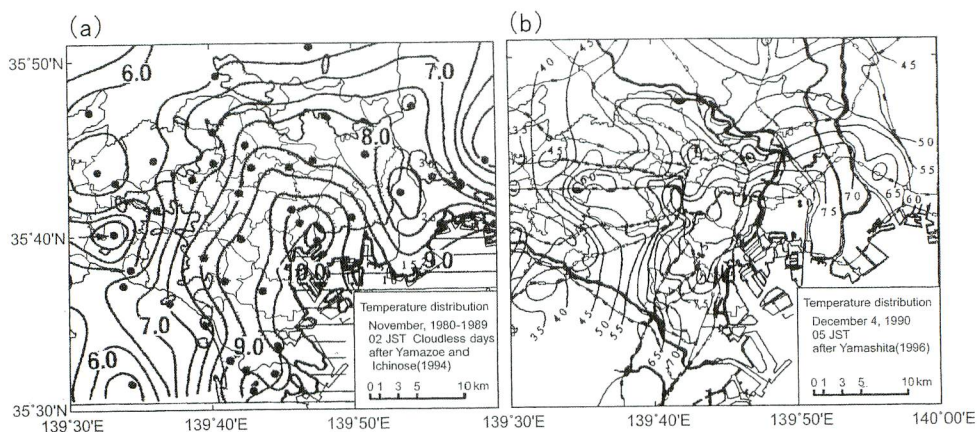


Fig. 9 Temperature distribution in the Tokyo wards area and its surroundings derived from observation data in 1980-1990 for clear-sky and weak-wind night (s). (a) At 02:00 JST in November of 1980-1989 (after Yamazoe and Ichinose, 1994), (b) At 05:00 JST on December 4, 1990 (after Yamashita, 1996). Contour lines are drawn every $0.5^{\circ}\text{C}/\text{h}$ in each figure.

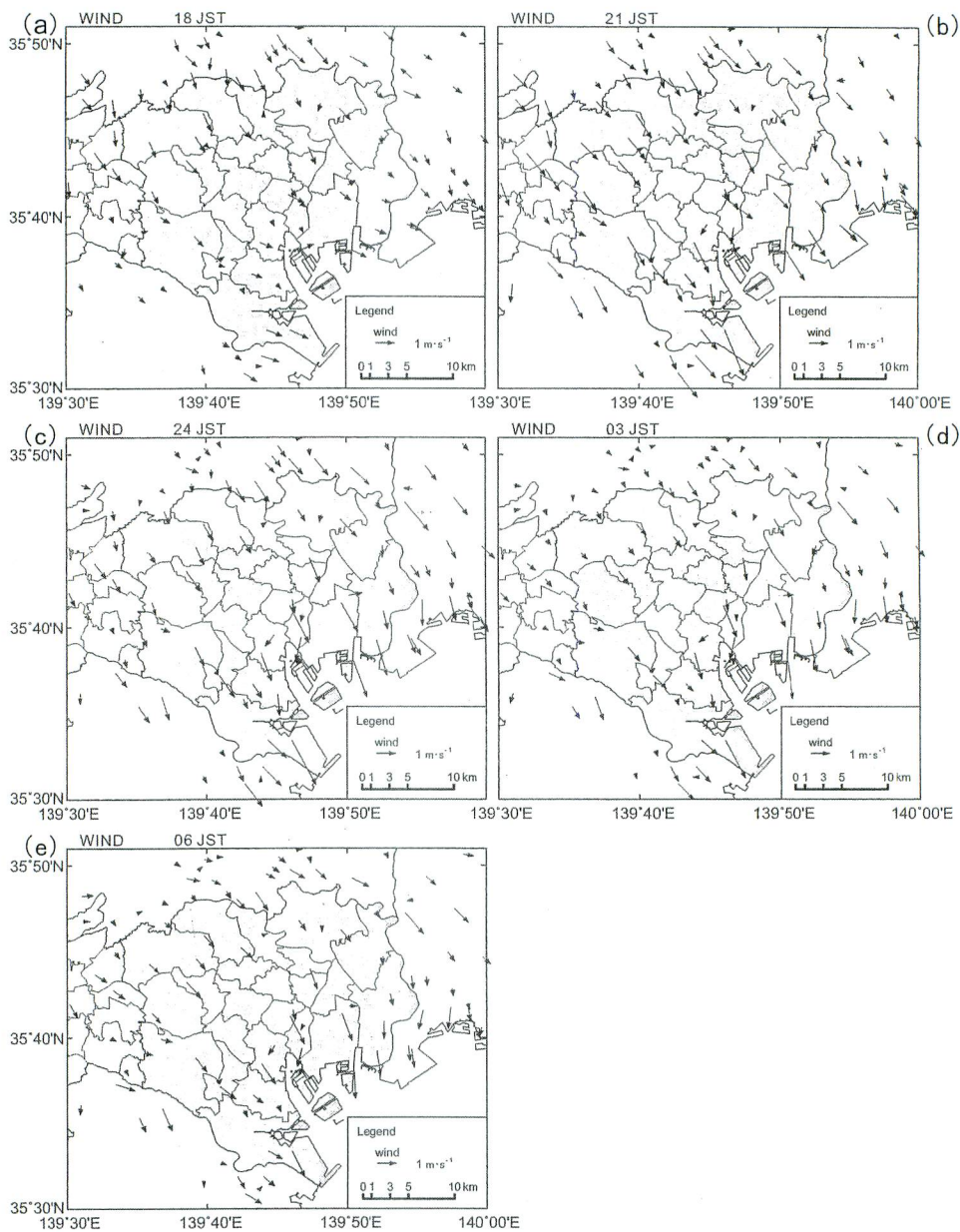


Fig. 10 Composite surface wind distribution in the Tokyo-ward area and its surroundings corresponding to Fig. 6.
 (a) 18:00 JST, (b) 21:00 JST, (c) 24:00 JST, (d) 03:00 JST, (e) 06:00 JST.

Reprinted from *Journal of Geography*. Vol. 132-(2), pp. 189~210, 2014.